



## RESEARCH ARTICLE OPEN ACCESS

# Transcriptional Signatures of the Right Ventricle in End-Stage Heart Failure

Jonah D. Garry<sup>1</sup> | Giovanni E. Davogusto<sup>1</sup> | Vineet Agrawal<sup>1,2</sup> | Fei Ye<sup>3</sup> | Kelsey Tomasek<sup>1</sup> | Yan Ru Su<sup>1</sup> | Tarek Absi<sup>4</sup> | James D. West<sup>5</sup> | Anna Hemnes<sup>5</sup> | Evan L. Brittain<sup>1</sup>

<sup>1</sup>Division of Cardiovascular Medicine, Vanderbilt University Medical Center, Nashville, Tennessee, USA | <sup>2</sup>Department of Veteran Affairs, Tennessee Valley Healthcare System, Nashville, Tennessee, USA | <sup>3</sup>Department of Biostatistics, Vanderbilt University Medical Center, Nashville, Tennessee, USA | <sup>4</sup>Department of Cardiac Surgery, Vanderbilt University Medical Center, Nashville, Tennessee, USA | <sup>5</sup>Division of Allergy, Pulmonary, and Critical Care Medicine, Vanderbilt University Medical Center, Nashville, Tennessee, USA

**Correspondence:** Evan L. Brittain ([evan.brittain@vumc.org](mailto:evan.brittain@vumc.org))

**Received:** 19 December 2024 | **Revised:** 10 April 2025 | **Accepted:** 16 April 2025

**Funding:** This study was supported by the National Heart Lung and Blood Institute.

**Keywords:** pulmonary hypertension | right ventricular failure | transcriptomics

## ABSTRACT

The molecular mechanisms driving right ventricular (RV) adaptation to stress and failure in end-stage heart failure (HF) are largely unknown. We aimed to characterize myocardial transcriptional changes in the RV caused by left sided HF and comparing RV compensation to failure. Additionally, we compared transcriptomic changes between right and left ventricular (LV) failure. Paired right and left ventricular myocardial tissue samples were obtained from 33 human subjects with end stage HF referred for transplantation and 8 control donors with unused transplant hearts. RV samples from end stage HF subjects were subdivided into compensated ( $n = 25$ ) and failing ( $n = 8$ ) categories based on pulmonary artery pulsatility index of  $< 1.85$ . All samples underwent bulk tissue RNA-sequencing. We compared gene expression between groups and performed pathway enrichment analysis. Pathways related to fatty acid metabolism and mitochondrial function were negatively enriched, while extracellular structure-related pathways were positively enriched in stressed RVs (compensated and failing) compared to controls. Compensated and failing RVs were differentiated by transcriptional changes in protein production/processing and immune system pathways. PPAR signaling and fatty acid metabolism pathways were consistently enriched in the RV compared to the LV. The RV has a distinct transcriptional signature under stress and in failure. Overlapping molecular mechanisms may underlie RV failure in pulmonary arterial hypertension and HF. Fatty Acid metabolism and associated signaling pathways appear enriched in the RV compared to the LV.

## 1 | Introduction

Right ventricular (RV) failure is common in left heart failure (HF) and associated with adverse outcomes [1–5], yet the molecular mechanisms underlying RV compensation and progression to failure are incompletely understood [6]. There are

currently no RV-specific biomarkers or medical therapies to address RV failure. The pathways thus far identified associating with RV failure derive predominantly from animal models and human studies of pulmonary arterial hypertension (PAH) with changes noted in inflammation [7–9], sex hormone expression [10, 11], cellular metabolism [12, 13], and extracellular matrix

Jonah D. Garry and Giovanni E. Davogusto are co-authors with equal contribution.

Guarantor: JG and EB are responsible for the overall content of the manuscript.

This is an open access article under the terms of the [Creative Commons Attribution-NonCommercial](https://creativecommons.org/licenses/by-nc/4.0/) License, which permits use, distribution and reproduction in any medium, provided the original work is properly cited and is not used for commercial purposes.

© 2025 The Author(s). *Pulmonary Circulation* published by Wiley Periodicals LLC on behalf of the Pulmonary Vascular Research Institute.

(ECM) organization [9, 14]. Multiple outstanding questions remain, including how these pathways relate to progression from RV compensation to failure, whether pathways associated with RV failure in PAH are also associated with RV failure in patients with HF, and to what degree the pathways identified are unique to the RV.

Myocardial transcriptomic analysis is a powerful tool for understanding molecular mechanisms of cardiac failure and has been used to understand cellular changes in the failing left ventricle (LV) [15]. In contrast, only two human studies have examined transcriptomic changes associated with RV progression from compensation to failure. These have focused on biomarker development—one in PAH and one in HF [14, 16]. No studies have directly compared transcriptional changes in RV failure compared to LV failure.

To address these gaps, we performed bulk RNA-sequencing of myocardial tissue to describe transcriptional changes in the RV that occur (1) In the context of stress from left-HF by comparison to controls and (2) As the RV progresses from compensation to failure. We further compared transcriptomic changes that occur in RV failure to the transcriptomic changes that occur in LV failure. We hypothesized that a comparison of the failing RV to the failing LV would yield insights into the unique and overlapping molecular mechanisms of ventricular failure.

## 2 | Methods

All procedures were reviewed and approved by the Vanderbilt Institutional Review Board # 090828 (biorepository registry) and 181788. All patients provided written informed consent for participation in the biorepository registry with sample collection and subsequent molecular analysis.

Myocardial tissue samples were obtained from the Vanderbilt Heart and Vascular Institute Biorepository. Hearts were obtained from patients diagnosed with American Heart Association Stage D HF who underwent an orthotopic heart transplant without regard for left ventricular systolic function or underlying HF etiology. We excluded any patients that had a left ventricular assist device before transplant, a prior heart transplant, congenital heart disease, or a clinically suspected hereditary cardiomyopathy. Samples without paired LV and RV tissue available were also excluded. Control samples were obtained from unmatched donor hearts that were not ultimately used for transplantation due to intravenous drug use, abnormal T waves during stroke, possible pericarditis, known coronary artery disease, and/or history of smoking. In all hearts, myocardial samples free of macroscopic fibrosis and epicardial fat were obtained from the RV and LV free-walls at 5–7 cm above the apex, flash frozen in liquid nitrogen and stored in  $-80^{\circ}\text{C}$  freezers. Control samples were dissected and immediately frozen in the operating room at the time of explant. For HF samples, the time from cross clamp to sample freezing (cold ischemic time) was available in 30 of the 33 subjects with HF, with a median time of 47 min (IQR: 38–60).

## 2.1 | RNA Extraction and Sequencing

Approximately 90–120 mg of tissue per ventricle per study subject was used for RNA extraction. Total RNA was isolated using the RNeasy miRNA Mini Kit and the QIAcube (Qiagen) for nucleic acid extraction following the manufacturer's instructions. Total RNA was submitted to the Vanderbilt VANTAGE Core for RNA sequencing. Sample quality and concentration of the total RNA were determined using the 2100 Bioanalyzer, RNA ScreenTape, and TapeStation Analysis Software A.02.02(SR1) (Agilent Technologies; Santa Clara, CA). For each library, approximately 100 ng of total RNA underwent ribosomal RNA depletion. Then, cDNA libraries were prepared using stranded mRNA (polyA-selected) with the TruSeq RNA Sample Prep Kit (Illumina; San Diego, CA) according to the manufacturer's instructions. Library quality was assessed with the 2100 Bioanalyzer. Sequencing was performed in a single batch, at a Paired-End 150 bp on the Illumina NovaSeq. 6000. RNAseq data were quality controlled repeatedly at raw, alignment, and expression levels [17]. QC3 was used for quality control of raw and alignment data [18]. Alignments were performed with Tophat 2 against the HG19 human reference genome [19]. Sequence data is available at the NCBI Short Read Archive.

## 2.2 | Group Definitions and Comparisons

Baseline demographics were collected for all patients. In HF patients, the laboratory, echocardiographic, and hemodynamic parameters closest to the time of transplant were recorded. We defined RV failure by a pulmonary artery pulsatility index (PAPi) of  $<1.85$ . We chose this definition based on a demonstrated clinical association between PAPi and adverse outcomes in end-stage HF [20–22] as well as evidence of RV myofilament contractile dysfunction at this cutoff [23]. We categorized myocardial samples into 5 mutually exclusive groupings: (1) Control RV ( $n = 8$ ); (2) Failing RV ( $n = 8$ ); (3) Compensated RV ( $n = 25$ ); (4) Control LV ( $n = 8$ ); (5) Failing LV ( $n = 33$ ). Definitions for each of these groupings are displayed in Supporting Information S1: Table S1.

We sought to understand myocardial transcriptional changes in the RV through four sets of comparisons. (1) We examined the RV under stress by comparing Control RV to Compensated RV and Control RV to Failing RV; (2) We described differences between the Compensated RV and Failing RV; (3) We compared transcriptional changes in RV failure to transcriptional changes in LV failure (comparing Failing RV vs Control RV to Failing LV vs Control LV). For this comparison we only included Failing LV samples from patients with concurrent RV failure; (4) We compared transcription between the RV and LV, examining differences between the ventricles separately in control and HF samples. An overview of the comparisons is displayed in Figure 1.

## 2.3 | RV-Specific Biomarker Candidates

We examined previously proposed biomarkers of RV failure from two prior myocardial transcriptomic studies for their

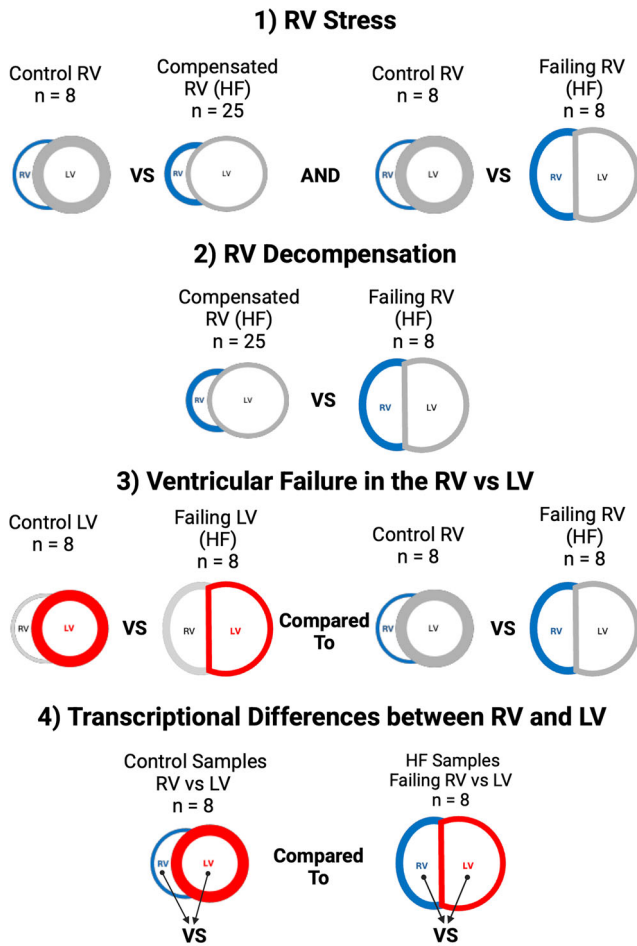


**FIGURE 1** | Overview of transcriptional comparisons. Displays an overview of the transcriptional comparisons performed: (1) We examined the RV under stress by comparing Control RV to Compensated RV and Control RV to Failing RV; (2) We described differences between the Compensated RV and Failing RV; (3) We compared transcriptional changes in RV failure to transcriptional changes in LV failure (comparing Failing RV vs. Control RV to Failing LV vs. Control LV). For this comparison we only included Failing LV samples from patients with concurrent RV failure; (4) We compared transcription between the RV and LV, examining differences between the ventricles separately in control and HF samples.

ability to discriminate between control, compensated, and failing RV samples. An optimal RV-specific biomarker would change minimally between normal LV and failing LV, therefore we compared whether normalized gene counts changed in both the RV and LV (comparing control to failing ventricles). To identify novel potential biomarkers of RV failure, we described the top 10 genes differentially expressed between failing and control RV, but not between failing and control LV.

## 2.4 | Statistical Analysis

Descriptive data are presented as counts and frequencies for categorical variables and quartiles for continuous variables unless otherwise specified. Raw count data was normalized and transformed to the log<sub>2</sub> scale before differential expression analysis using the R package DESeq. 2 [24]. Dispersion

estimates plots were visually inspected to ensure appropriate fit of the negative binomial model. To visualize the separation of groups we performed unsupervised clustering analyses via principal components analysis (PCA) and supervised clustering by partial least squares discriminant analysis (PLS-DA) to maximize separation. We identified differentially expressed genes (DEGs) based on a Benjamin-Hochberg false discovery rate (FDR) adjusted *p*-value of < 0.05 and an absolute log fold change of 0.5 or greater. We performed functional analysis using Overrepresentation Analysis (ORA) on gene sets of interest and compared between groups using gene set enrichment analysis (GSEA) on the WEB-based Gene Set AnaLysis Toolkit (WebGestalt) 2024 [25]. For ORA and GSEA, we selected the top 20 KEGG pathways and Gene Ontology Biological Processes with FDR-adjusted *p*-value of < 0.10, excluding KEGG pathways for non-cardiac disease-specific processes (i.e., pathways for “Alzheimer Disease” or “Leishmaniasis”). For biomarker assessment, we identified genes with significantly different normalized counts based on a Bonferroni-adjusted *p*-value of < 0.05 divided by number of biomarkers assessed. All statistical analyses were performed with the R software program, version 4.3.3.

## 3 | Results

### 3.1 | Patient Characteristics

We included 33 subjects with AHA stage D HF and 8 controls from the Vanderbilt Heart and Vascular Institute Biorepository. Subjects with HF were older at harvesting (52.7 years vs. 43.5 years) with a higher proportion of males (64% vs. 50%). Other than age, clinical characteristics are not available for control subjects. Laboratory, echocardiographic, and hemodynamic parameters closest to transplant for the HF group are displayed in Table 1. HF etiology was non-ischemic in 21 subjects (64%) and ischemic in 12 subjects (36%). The median BNP was 454 (IQR: 261–1400). On average, transthoracic echocardiograms were conducted 54 days (IQR: 16–133) before transplant, and hemodynamics were obtained 20 days (IQR: 6–40) before transplant. Median LVEF was 19% (IQR: 15–27), mean pulmonary artery pressure was 27 mmHg (IQR: 20–35), and pulmonary capillary wedge pressure was 17 mmHg (IQR: 11–23). Nearly all patients were receiving inotropes before transplant (*n* = 32 [97%]) and a minority were supported with an intra-aortic balloon pump (*n* = 7 [21%]).

Eight subjects (24%) had RV failure based on PAPI < 1.85. Subjects with RV failure and those with compensated RV function were similar in age, sex distribution, and BMI. All subjects with RV failure had non-ischemic cardiomyopathy, whereas among those with compensated RV function, 13 (52%) had non-ischemic cardiomyopathy and the remainder had ischemic cardiomyopathy. Qualitative RV dilation and RV systolic dysfunction were more common in the RV failure group. The median PAPI of subjects with RV failure was 1.37 (IQR: 0.68–1.69) compared to 4.50 (IQR: 3.40–6.00) among subjects with RV compensation. Subjects with RV failure also had a higher median RA/PCWP ratio compared to subjects with RV compensation (0.78 [IQR: 0.62–0.85] vs. 0.34 [IQR: 0.22–0.45], *p* < 0.001).

**TABLE 1** | Baseline clinical characteristics of the patients with end-stage HF.

Characteristic	Overall HF cohort (n = 33)	Failing RV (n = 8)	Compensated RV (n = 25)
Age	52.7 (61.0–44.0)	55.6 (46.7–62.6)	52.7 (43.7–60.9)
Male gender	21 (64%)	5 (62%)	16 (64%)
BMI	26.5 (24.3–30.4)	26.3 (23.1–28.5)	26.5 (24.4–30.4)
Race/ethnicity			
White	26 (79%)	6 (75%)	5 (20%)
Black	7 (21%)	2 (25%)	20 (80%)
Etiology			
Ischemic	12 (36%)	0 (0%)	12 (48%)
Non-ischemic	21 (64%)	8 (100%)	13 (52%)
Transplant listing status			
Status 1A	10 (30%)	3 (38%)	7 (28%)
Status 1B	21 (64%)	5 (62%)	16 (64%)
Status 2	2 (6%)	0 (0%)	2 (8%)
Pre-transplant support			
Milrinone	32 (97%)	8 (100%)	24 (96%)
IABP	7 (21%)	1 (13%)	6 (24%)
Laboratory			
BNP (pg/mL)	454 (261–1400)	302 (147–1110)	503 (283–1440)
Creatinine (mg/dL)	1.3 (1.0–1.5)	1.4 (1.2–1.7)	1.3 (1.0–1.5)
Sodium (mEq/L)	138 (136–138)	138 (136–139)	138 (136–138)
Echocardiographic			
Days before sample	54 (16–133)	75 (41–99)	40 (16–134)
LVIDd (cm)	6.1 (5.4–6.9)	6.3 (5.5–7.1)	6.1 (5.4–6.7)
IVSD (cm)	0.9 (0.8–1.0)	0.8 (0.8–0.9)	0.9 (0.8–1.0)
LVPWD (cm)	1.0 (0.8–1.1)	0.9 (0.8–1.0)	0.9 (0.8–1.0)
LVEF	19 (15–27)	15 (15–16)	22.3 (18–28)
RV dilation (qualitative)			
Normal	24 (73%)	4 (50%)	20 (80%)
Mild	6 (18%)	2 (25%)	3 (16%)
Moderate+	3 (9%)	2 (25%)	1 (4%)
RV systolic function (qualitative)			
Normal	17 (52%)	5 (63%)	20 (80%)
Mild	8 (24%)	0 (0%)	4 (16%)
Moderate +	8 (24%)	3 (37%)	0 (0%)
Hemodynamics			
Days before sample	20 (6–40)	14 (4–46)	20 (9–40)
RA mean (mmHg)	6 (3–13)	14 (13–16)	5 (2–7)
PA systolic (mmHg)	39 (31–50)	42 (38–46)	37 (39–51)
PA diastolic (mmHg)	18 (12–23)	23 (20–30)	14 (10–20)
PA mean (mmHg)	27 (20–35)	33 (27–36)	27 (19–33)
PCWP (mmHg)	17 (11–23)	22 (17–25)	17 (10–22)
Cardiac output (L/min)	4.4 (3.8–5.1)	4.8 (4.1–6.0)	4.1 (3.6–5.0)
Cardiac index (L/min/m <sup>2</sup> )	2.3 (2.1–2.8)	2.4 (2.1–3.0)	2.2 (2.2–2.7)

(Continues)

**TABLE 1** | (Continued)

Characteristic	Overall HF cohort (n = 33)	Failing RV (n = 8)	Compensated RV (n = 25)
PVR (woods units)	2.5 (2.0–3.1)	2.6 (2.3–2.8)	2.4 (2.0–3.1)
PAPi	3.8 (2.1–6.0)	1.4 (0.7–1.7)	4.5 (3.4–6.0)

Abbreviations: BNP, B-type natriuretic peptide; DBP, diastolic blood pressure; IVSd, interventricular septal wall in diastole; LVEF, left ventricular ejection fraction; LVIDd, left ventricular internal diameter in diastole; LVPWd, left ventricular posterior wall in diastole; MAP, median arterial pressure; PA, pulmonary artery; PCWP, pulmonary capillary wedge pressure; PVR, pulmonary vascular resistance; RA, right atrium; RV, right ventricle; SBP, systolic blood pressure; SVR, systemic vascular resistance; TAPSE, tricuspid annular plane systolic excursion.

### 3.2 | Transcriptomic Features of the Right Ventricle Under Stress in End-Stage HF

Principal component analysis revealed clear separation between the RV under stress (Compensated RV and Failing RV) compared to Control RV samples, but poorly differentiated between Compensated RV and Failing RV (Figure 2A). PLS-DA further supported a distinct separation between the RV under stress and control samples with an improved differentiation between Failing and Compensated RV samples (Figure 2B).

We identified 2696 DEGs (1362 with increased counts and 1334 with decreased counts) comparing Compensated RV versus Control RV and 2180 DEGs (1111 with increased counts and 1069 with decreased counts) comparing Failing RV versus Control RV (Figure 2C,D). There were 870 genes with increased counts in both comparisons (increased transcription in the RV under stress). The top 10 genes were MXRA5, PHLDA1, SMOC2, GPRASP2, SDSL, NHSL1, GPRASP1, PHLDB2, KIAA0141, and XPO4. On ORA, the 870 genes most prominently mapped to the pathways of Extracellular Structure Organization and External Encapsulating Structure Organization (Figure 3A). There were 863 genes with decreased counts shared in both comparisons, representing a gene set with decreased transcription in the RV under stress. The top 10 genes with decreased counts in the RV under stress were AOX1, AKR1C1, FCN3, CD38, HMOX2, TGFBR2, GNMT, MARK3, NT5DC2, and JTB. On ORA, these 863 genes most prominently mapped to Metabolic Pathways, including Fatty Acid Metabolic Process, Organic Acid Biosynthetic Process, and Icosanoid Metabolic Processes among others (Figure 3B). Of note, pathways related to immune system function were enriched among both overlapping gene sets with increased and decreased counts.

The top 20 pathways identified on GSEA for the comparisons between Failing RV versus Control RV and Compensated RV versus Control RV are shown in Figure 3C. In the RV under stress, there was negative enrichment of pathways related to protein processing and production (Ribosome, Proteasome, Endoplasmic Reticulum Organization), fatty acid metabolism (Icosanoid Metabolic Process, Response to Lipoprotein Particle, Cellular Response to Lipoprotein Particle Stimulus, Response to Fatty Acid), mitochondrial function (Mitochondrial Gene Expression, Reactive Oxygen Species Metabolic Process, Respiratory Burst) and macrophage function (Phagosome, Foam Cell Differentiation), with positive enrichment of pathways related to hedgehog signaling and circadian rhythm.

### 3.3 | Transcriptomic Features of RV Progression From Compensation to Failure

We then compared transcript counts between the failing RV and compensated RV groups defined by the PAPi cutoff of 1.85. The top 10 DEGs were CXCL11, CD209, LOX, SLC25A23, WDR49, EFHC2, COL6A6, LDB3, NFIC, and CA3. Of these only CXCL11, a chemokine, reached our multiple comparison testing and log-fold change significance threshold. We then performed GSEA to identify differentially enriched pathways with the top 20 pathways displayed in Figure 4A,B. RV failure was negatively enriched in the Ribosome, Proteasome, Cytoplasmic Translation, and Cellular Component Assembly Involved in Morphogenesis pathways, and positively enriched in pathways related to inflammation including Response to Protozoan, Complement and Coagulation Cascades, IL-2 Production, and Response to Type II Interferon, among others.

We evaluated whether previously suggested biomarkers of RV failure effectively differentiated between RV control, compensated, and failing samples in our cohort. We assessed the difference in average normalized counts for the ECM and cell adhesion genes CRTAC1, MEGF9, C1QTNF1, ITGAM, NID1, SPARCL1, TGFBR3, and FAP identified by Khassafi et al. [14] and eight additional proposed biomarkers of RV failure identified by Di Salvo et al. [16] including SERPINA3, SERPINA5, LCN6, LCN10, STEAP4, ARK1C1, STAC2, VSIG4. We found that none of the genes effectively differentiated between failing and compensated RV, however, all except CRTAC1 and MEGF9 did effectively differentiate between RV under stress and RV controls (Supporting Information S1: Figure S1).

### 3.4 | Transcriptomic Features of Ventricular Failure Compared Between the Right Ventricle and LV

To understand which transcriptional changes were unique to RV failure in comparison to LV failure we next compared DEGs in RV failure (Failing vs. Control RV) and LV Failure (Failing vs. Control LV). There were 1785 DEGs (791 with decreased counts in failure and 994 with increased counts in failure) comparing the failing and control LV in patients who had concurrent RV failure (Supporting Information S1: Figure S2). Of the 791 DEGs with decreased counts in LV failure, 487 genes were also decreased in RV failure. These genes mapped most prominently to Metabolic Pathways, Complement and Coagulation Cascades, One-Carbon Metabolic Process, Vascular Process in Circulatory System, and HIF-1 Signaling Pathway (Figure 5A). There were 561 overlapping genes with increased



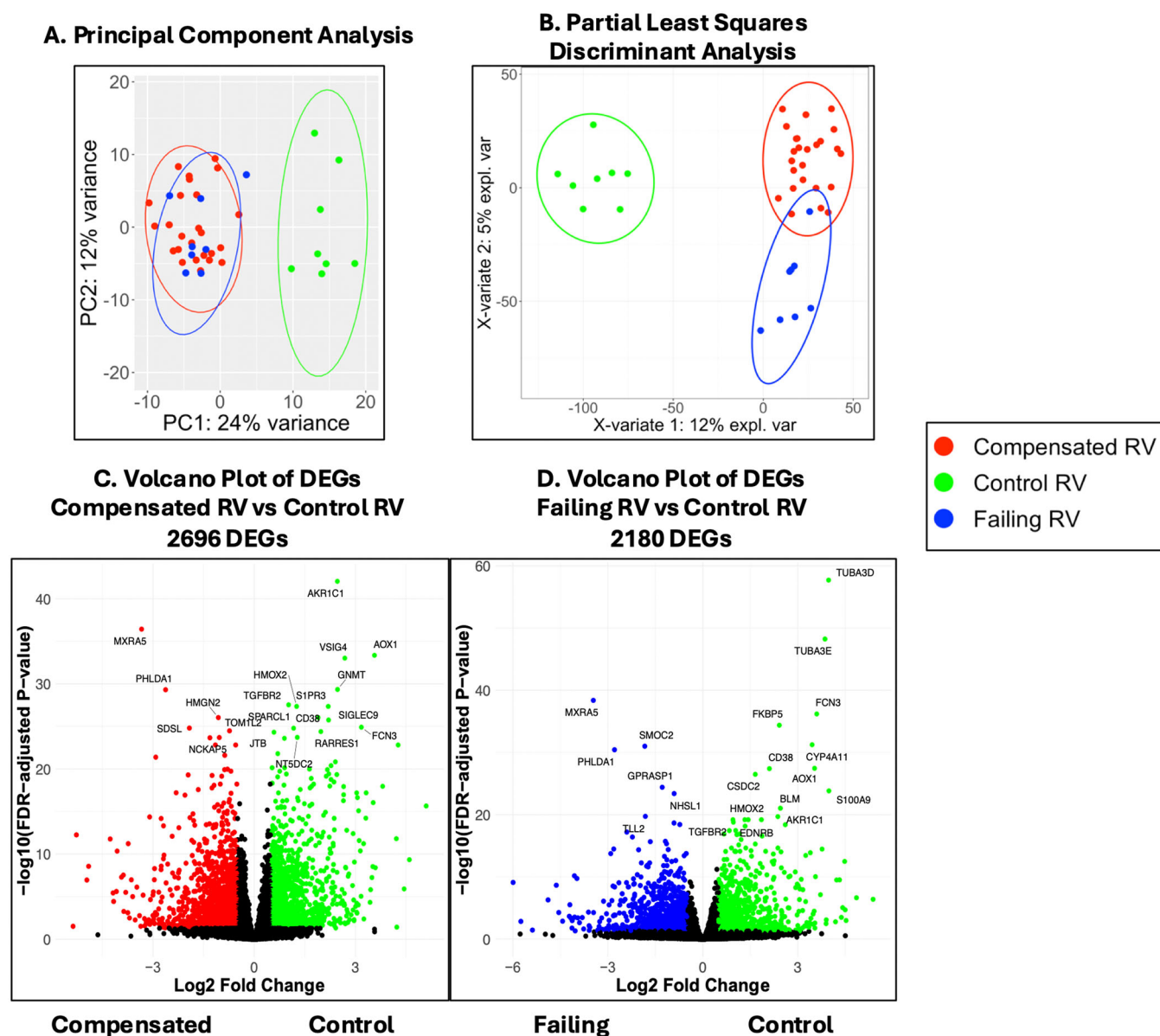
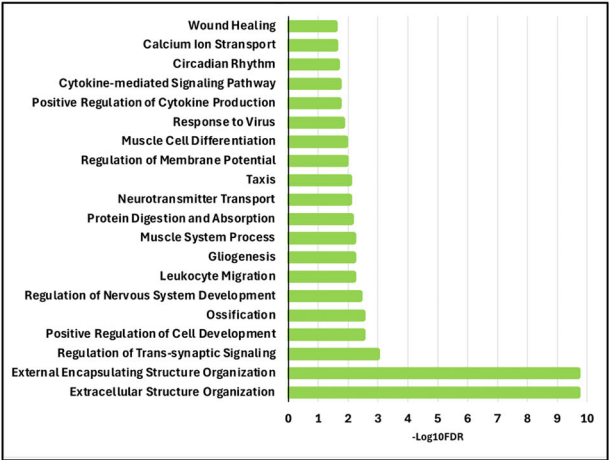


**FIGURE 2** | (A–D) Gene expression in the right ventricle under Stress. (A) Displays separation between failing, compensated, and control RV samples by the first two principal components. On principal component analysis (PCA) there is clear separation between compensated RV samples (red) and control RV samples (green) as well as between failing RV samples (blue) and control samples, however there is poor separation between compensated and failing RV samples. (B) Displays partial least squares discriminant analysis (PLS-DA) based separation between RV sample groups. There is clear separation between control RV samples (green) and compensated RV samples (blue) as well as between control RV samples and failing RV samples (red). PLS-DA based separation between compensated and failing RV samples is significantly improved from PCA. (C) Displays a Volcano plot for the differentially expressed genes (DEG) comparing between control and compensated RV samples. Genes in green are more highly expressed in control RV samples, while genes in red are more highly expressed in compensated RV samples. (D) Displays a Volcano plot for the DEGs comparing between control and failing RV samples. Genes in green are more highly expressed in control RV samples, while genes in blue are more highly expressed in failing RV samples.

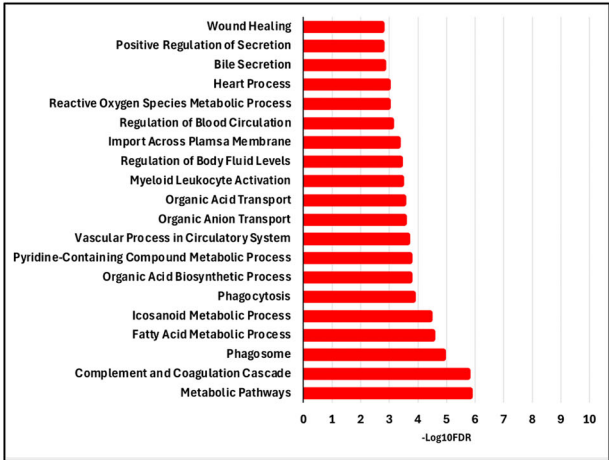
counts in both RV and LV failure compared to respective controls. These genes mapped most prominently to Extracellular Structure Organization and External Encapsulating Structure Organization (Figure 5B). We then compared GSEA-identified pathways in the failing vs control RV and the failing vs control LV (Figure 5C). Failing samples in both ventricles were negatively enriched in pathways related to protein transcription and translation (Ribosome, Proteasome, Cytoplasmic Translation, Protein Processing in Endoplasmic Reticulum) as well as mitochondrial function (Cell Redox Hemostasis, Mitochondrial

Gene Expression) and positively enriched in Hedgehog Signaling. Unique to failure in the RV, there was negative enrichment of pathways related to fatty acid metabolism and cellular response to lipoprotein/fatty acid (Icosanoid Metabolic Process, Response to Lipoprotein Particle, Cellular Response to Lipoprotein Particle Stimulus, Response to Fatty Acid). GSEA-identified pathways unique to LV failure included negative enrichment of cellular metabolism related gene sets, including Mitochondrial Function (Oxidative Phosphorylation, Mitochondrial Transport, Protein Localization to Mitochondrion,

**A. Pathways Enriched - Increased Expression in RV**



**B. Pathways Enriched - Decreased Expression in RV Stress**

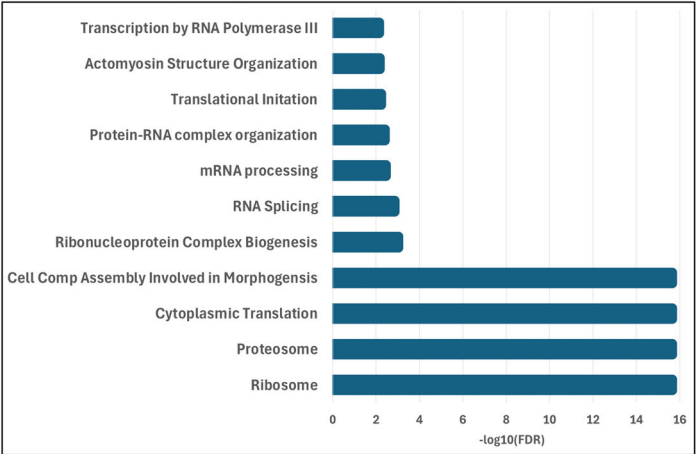


**C. Gene Set Enrichment Analysis in RV stress (Failing & Compensated RV) compared to Control RV**



**FIGURE 3** | (A–C) Pathways enriched in the right ventricle under stress. (A and B) Display the top 20 pathways enriched among genes with increased expression in RV stress (A) and decreased expression in RV stress (B). (C) Displays the top 20 pathways identified on gene set enrichment analysis from the comparisons between failing RV vs control RV (first column) and compensated RV vs control RV (second column). The positively enriched pathways in RV stress are displayed in green, while negatively enriched pathways in RV stress are displayed in red.

**A. Negatively Enriched Pathways in Failing RV**



**B. Positively Enriched Pathways in Failing RV**

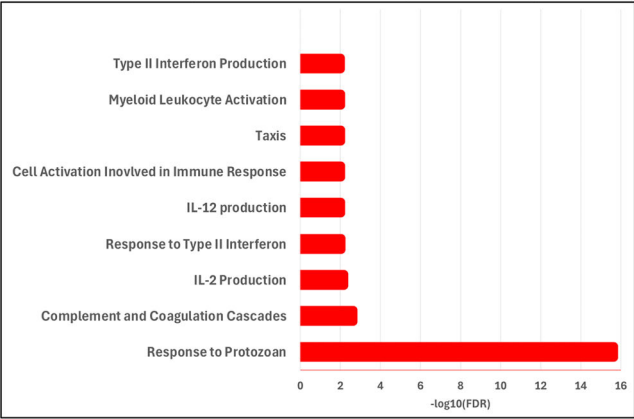


**FIGURE 4** | Pathways enriched in RV failure. Displays the top 20 pathways identified on gene set enrichment analysis when comparing failing right ventricle (RV) samples to compensated RV samples. (A) Displays pathways that were negatively enriched in the Failing RV. (B) Displays the pathways that were positively enriched in the Failing RV.



**FIGURE 5** | Pathway enrichment in right ventricular and left ventricular failure. (A) Displays the enriched pathways among the 487 genes with decreased expression in both right ventricular (RV) and LV failure compared to respective controls. (B) Displays the top 20 pathways among the 561 genes with increased expression in both RV and LV failure compared to respective controls. (C) Displays the top 20 gene set enrichment analysis identified pathways from the comparisons between failing RV vs control RV (first column) and failing LV versus control LV (second column). Pathways that are positively enriched in failure are displayed in green, while pathways that are negatively enriched in failure are displayed in red.

Electron Transport Chain), Glycolysis/Gluconeogenesis, Insulin Signaling Pathway, and protein transcription and translation (Translation Initiation, Protein Neddylolation). However, many of the overarching processes were also implicated in RV failure through different KEGG/GO pathways (Mitochondrial Function, and protein transcription and translation).

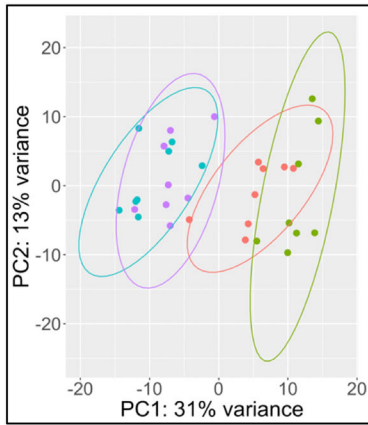
### 3.5 | Transcriptomic Differences Between the Right and LVs

We then sought to understand which genes and pathways differentiated the RV from the LV in control subjects and HF subjects with biventricular failure. PCA demonstrated good separation between failing and control ventricular samples but did not effectively differentiate between RV and LV samples (Figure 6A). Discrimination improved using PLS-DA (Figure 6B). We identified 357 DEGs comparing Control RV to Control LV (Figure 6C) and 109 DEGs comparing Failing RV to Failing LV (Figure 6D). Of these, 36 genes overlapped in both comparisons, representing a gene set that differentiates RV from LV in both control and failure. These genes were most prominently found in metabolism-related pathways including PPAR signaling

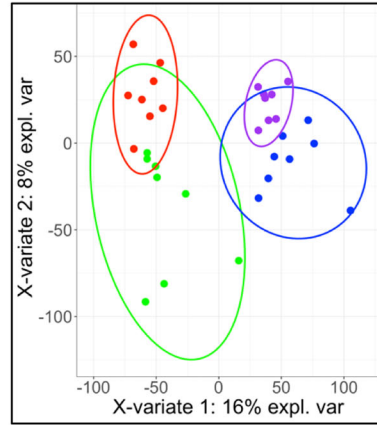
(ADIPOQ, ANGPTL4, PCK1;  $p_{adj} = 0.12$ ), Adipocytokine signaling (ADIPOQ, PCK1, POMC;  $p_{adj} = 0.12$ ), carbohydrate biosynthetic process (ADIPOQ, PCK1, GPD1, RBP4;  $p_{adj} = 0.15$ ), and lipid localization (ADIPOQ, C3, POMC, PRELID2, RBP4;  $p_{adj} = 0.26$ ). By average rank, the top 10 genes differentiating RV and LV regardless of control or failure were CFD, FAIM2, GRXCR2, IGSF10, RBP4, LYVE1, SNAP91, COL28A1, SLC19A3, and DPP6. GSEA comparing RV to LV in both control and failing ventricular myocardium revealed two overlapping pathways, indicating that PPAR signaling and Fatty Acid Metabolism were positively enriched in RV samples compared to LV samples regardless of control or failing status (Figure 7). Unique to the failing RV compared to the failing LV, there was a positive enrichment of pathways related to protein translation and processing (Ribosome, Proteasome, Protein Processing in Endoplasmic Reticulum, Protein Export, Cytoplasmic Translation, Translational Initiation, Protein Neddylolation) and mitochondrial function (Oxidative Phosphorylation, Pyruvate Metabolism, Electron Transport Chain, Mitochondrial Gene Expression, Energy Derivation by Oxidation of Organic Compounds, NADH Dehydrogenase Complex Assembly). In contrast, unique to the control RV compared to the control LV there was positive enrichment of inflammation related gene sets.



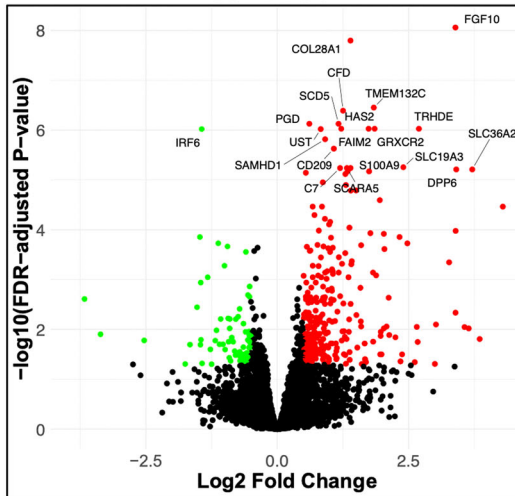
## A. Principal Component Analysis



## B. Partial Least Squares Discriminant Analysis

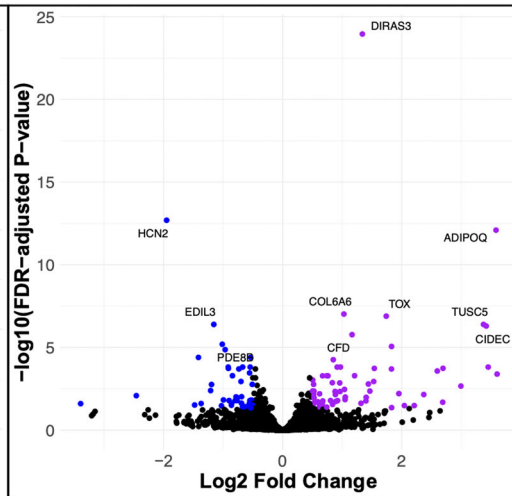


## C. Volcano Plot of DEGs Control RV vs Control LV 357 DEGs



Left Ventricle Right Ventricle

## D. Volcano Plot of DEGs Failing RV vs Failing LV 109 DEGs



Left Ventricle Right Ventricle

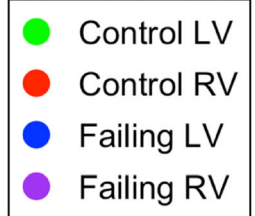


**FIGURE 6** | Gene expression and pathway enrichment in right versus left ventricle. (A) Displays separation between control RV (red), failing RV (purple), control LV (green), and failing LV (blue) samples by the first two principal components. There is clear separation between Control and Failing samples, but separation is less clear between RV and LV samples. (B) Displays partial least squares discriminant analysis (PLS-DA) between control RV (red), failing RV (purple), control LV (green), and failing LV samples (blue). Separation between control and failing ventricular samples remains robust, with improved separation between RV and LV samples. (C and D) Display a Volcano plot for the differentially expressed genes (DEG) comparing between the RV and LV in controls (C) and in failure (D).

Lastly, we assessed whether previously suggested biomarkers of RV failure from Khassafi et al. [14] and Di Salvo et al. [16] were unique to differentiating between RV failure and RV control or also varied between LV failure and LV control. Of the 16 genes, SPARCL1, TGFBR3, FAP, SERPINA5, and ARK1C1 were differentially expressed between the failing RV and control RV, but not the failing LV and control LV (Supporting Information S1: Figure S3). In our study, the top 10 genes that were differentially expressed in the failing RV compared to control RV without differential expression in the failing LV compared to control LV were WASF3, SHB, PATZ1, TRPC6, SPTSSA, IFT43, ART4, LGI3, CTF1, and CPT2 (Supporting Information S1: Figure S4). There were no clear KEGG or GO pathways that included multiple genes. Some of these genes could be broadly

characterized as associated with lipid metabolism (AKR1C1, CPT2, SPTSSA), cell-cell signaling (TGFBR3, CTF1, LGI3, SHB, ART4, and IFT43), immune function (WASF3, TGFBR3, ART4, SERPINA5), and ECM remodeling (SPARCL1, TGFBR3, FAP, SERPINA5).

## 4 | Discussion

In this study, we performed bulk myocardial RNA-sequencing of paired LV and RV samples from patients with end-stage HF and controls. We then employed transcriptomic analyses including differential gene expression and enrichment analysis to identify changes in the RV under stress and to distinguish

## A. Gene Set Enrichment Analysis of RV vs LV Samples in Control and Failing Ventricles

KEGG/GO Pathway	Control Ventricles	Failing Ventricles
	RV vs LV	
Fatty Acid Metabolism		
PPAR Signaling		
Ribosome		
Valine, Leucine, Isoleucine Degradation		
Oxidative Phosphorylation		
Pyruvate Metabolism		
Fatty Acid Degradation		
Proteasome		
Propanoate Metabolism		
Protein Processing in Endoplasmic Reticulum		
Protein Export		
Ferropoptosis		
Cytoplasmic Translation		
Electron Transport Chain		
Translational Initiation		
Mitochondrial Gene Expression		
Energy Derivation by Oxidation of Organic Compounds		
Ribonucleoprotein Complex Biogenesis		
Protein Neddylation		
NADH Dehydrogenase Complex Assembly		
Response to Fatty Acid		
Acute Inflammatory Response		
IL-12 Production		
Regulation of Inflammatory Response		
Humoral Immune Response		
IL-8 Production		
Phagocytosis		
Urogenital System Development		
VEGF production		
Response to Fungus		
Chronic Inflammatory Response		
Response to IL-1		
TNF Superfamily Cytokine Production		
IL-10 Production		
Complement and Coagulation Cascades		
Hematopoietic Cell Lineage		
Phagosome		
Cellular Component Assembly Involved in Morphogenesis		
Inclusion Body Assembly		
Muscle Cell Cellular Homeostasis		

**Unique to Failure**

**Unique to Controls**

	Enriched in RV, FDR $p < 0.05$
	Enriched in RV, FDR $p < 0.10$
	Enriched in LV, FDR $p < 0.05$
	Enriched in LV, FDR $p < 0.10$

**FIGURE 7** | Displays the top 20 pathways identified on gene set enrichment analysis from the comparisons between RV and LV in control samples (first column) and failing samples (second column). The pathways enriched in the RV are displayed in blue, while the pathways enriched in the LV are displayed in red.

between compensation and failure. We compared these findings to the transcriptional changes in LV failure and assessed differences in the transcriptional signatures of the RV and LV. The major findings are: (1) The RV myocardium under the stress of LV failure exhibits transcriptional changes similar to those identified in PAH related RV failure, (2) Gene sets related to

inflammation and protein production/processing differentiate between compensated RV and failing RV, (3) PPAR signaling and fatty acid metabolism gene sets are consistently enriched in the RV compared to the LV regardless of control or failure status. Moreover, fatty acid metabolism is implicated as the primary differentiator between transcriptomic signatures of RV

failure and LV failure, (4) The transcriptional profile of the control RV features prominent enrichment of inflammation and immune system pathways compared to the LV, (5) We identify potential transcriptomic biomarkers of RV failure that are specific to the RV. These findings identify unique biology and pathology in the human RV and may contribute to the development of RV-specific biomarkers and therapeutics in HF, the most common cause of RV failure.

The transcriptional changes in RV tissue of end-stage HF subjects compared to controls suggest that similar molecular mechanisms may underlay RV failure in both PAH and end-stage HF. Comparable myocardial transcriptomic studies in human PAH and multiple animal models that recapitulate PAH via pre-capillary pulmonary hypertension (pulmonary artery banding, Sugen/Hypoxia, and Monocrotaline) have consistently identified an association between RV failure and increased expression of genes related to ECM remodeling, decreased expression of genes related to fatty acid metabolism and mitochondrial function, and variable change in expression of genes related to inflammation [14, 26–28]. Furthermore, targeted investigations have validated that these transcriptional changes correspond to increased ECM protein expression [14, 29], impaired fatty acid oxidation [13, 30], and dysregulated inflammation [7] in human subjects along with decreased mitochondrial function in rats [31]. Although transcriptomic findings must be validated as translating to protein expression, our findings suggest that molecular pathways identified in PAH may also be areas for the development of biomarkers and therapeutics in HF-associated RV failure.

Our study is unique compared to many prior transcriptomic investigations of RV failure in attempting to discriminate between the compensated and failing RV, with several strengths over the few prior studies examining this question. Two studies have examined RV transcriptomic changes comparing compensated and failing RV in patients with end-stage LV failure, finding few DEGs [16, 32]. The first was conducted in 22 subjects with end-stage HF and defined RV failure solely by echocardiographic variables with few patients meeting hemodynamic criteria and substantial time between echocardiogram and explant (mean:  $98 \pm 85$  days) [16]. The second included only 6 subjects with an LV assist device in place and employed solely hemodynamic criteria (elevated right sided filling pressure [ $> 18$  mmHg] and low cardiac index [ $< 2.0$  L/min/m<sup>2</sup>]), further categorizing severity by the need for inotropic or mechanical support [32]. One other study performed RNA-seq on human compensated RV samples from 15 subjects with congenital heart disease obtained at biopsy, confirmed to have normal RV function by cardiac index ( $> 2.2$  L/min/m<sup>2</sup>) and tricuspid annular plane systolic excursion (17 mm), comparing these to failing RV samples from 11 subjects with PAH obtained at autopsy [14]. They identified 260 DEGs that implicated enrichment of mitochondrial function associated pathways, however, these results may be biased by inherent differences in myocardial transcription between congenital heart disease and PAH. In contrast, our study was the largest to date with 33 subjects and employed a robust clinically and pathologically validated hemodynamic definition of RV failure that was obtained shortly before explant. Similar to the studies conducted in end-stage HF, we found few DEGs but present new

GSEA findings that implicate protein transcription and translation pathway enrichment in RV compensation and cytokine production/signaling as well as leukocyte activation pathway enrichment in RV failure. The limited differential gene expression noted in our study and prior investigations may relate to the criteria employed to differentiate between compensated and failing RV, limited sample sizes, or the heterogeneity of subjects.

The second unique aspect of our study was the direct comparison of transcriptional changes in RV failure and LV failure using paired RV and LV samples from control subjects and subjects with objectively defined biventricular failure. Although prior studies have separately examined transcriptional changes in RV failure and LV failure, the findings from separate studies are challenging to consolidate due to differing definitions of RV failure, clinically heterogeneous populations, and differences in analytic strategies. Given the differences in embryological origin and physiological pump conditions of the right and LV [33], we expected to find transcriptional differences. There was a notable enrichment of gene sets related to lipid signaling and metabolism in RV failure that was not noted in the LV failure. In addition, transcriptional differences between the RV and LV in both control and failure comparisons identified Fatty Acid metabolism, PPAR signaling, and Adipocytokine signaling as pathways enriched in the RV compared to LV. These findings suggest constituent differences between RV and LV metabolism involving fatty acids and associated metabolic regulatory signaling with changes to fatty acid metabolism that affect the RV in failure more prominently than the LV. Dysregulation of fatty acid metabolism is strongly implicated in RV failure related to PAH [6, 13, 30, 34] and in LV failure [35], however, fatty acid oxidation exhibits variable change in the failing LV, while it is consistently decreased in PAH-associated RV failure. Considered altogether, these findings suggest that certain changes to fatty acid metabolism and related signaling may be unique to the RV and potential areas for RV-specific biomarker development. We found that failure in both ventricles was associated with mitochondrial dysfunction, decreased protein transcription and translation, and changes to cellular metabolism, aligning with prior studies [14, 36]. We also noted enrichment of sonic hedgehog signaling in both RV and LV failure, a pathway that has not been noted in transcriptomic studies but has been implicated in cardiac regeneration and endothelial cell activation following injury [37–39].

Direct comparison of transcriptional profiles between the RV and LV in controls and failure identified enrichment of inflammation and immune function as the predominant differentiating pathway in the control ventricles and mitochondrial function as the predominant differentiating pathway in the failing ventricles. Inflammation and immune function related pathways were enriched in the control RV compared to LV, which may be due to transcriptional differences, but may be related to differential cell composition as animal studies have demonstrated a higher proportion of macrophages in the RV than the LV [40]. There is evidence that a dysfunctional immune system with myocardial inflammation plays a role in both ventricles when failing [41, 42], however, whether these changes are similar in the failing RV and failing LV remains an outstanding question. Mitochondrial function related pathways

were enriched in the failing RV compared to the failing LV. Rodent bioenergetic studies suggest increased oxygen consumption due to increased fatty acid oxidation in the normal RV cardiomyocytes compared to LV cardiomyocytes [43], however, we did not find a transcriptional difference in mitochondrial function related pathways comparing human control RV to control LV. Mitochondrial dysfunction may play a relatively less significant role in RV failure compared to LV failure. However, there are no metrics to directly compare the degree of dysfunction in the RV and LV and this difference in expression may be related to a greater degree of “failure” in LV samples compared to RV samples. Further, we would note that this difference in degree of “failure” may affect the findings from all comparisons between RV and LV tissue.

Development of an RV failure-specific biomarker in subjects with LV failure presents a unique challenge given the overlap in pathophysiology between the ventricles. We found that most previously suggested biomarkers for RV failure demonstrated a parallel change when comparing failing and control LV samples, suggesting that these biomarkers were not specific to the RV and therefore likely to be affected by functional changes to both ventricles. Our study identified 13 genes that are plausibly associated with RV failure and are differentially expressed in RV failure, but not LV failure. Ultimately, these genes and the pathways implicated may correlate with measurable plasma levels of transcript, protein, or metabolite that can specifically identify RV failure in patients with HF from LV failure. The proposed biomarkers require robust prospective validation before their clinical utility is established.

## 4.1 | Limitations

As our study employed bulk tissue RNA-sequencing, we are not able to determine the relative contribution of different cell types or compare transcription between individual cell types in each ventricle, both of which are factors that likely contribute to tissue function. Transcriptomic based analysis leverages relative transcript counts for biological inferences, which ultimately may not translate to protein expression or cellular/tissue function, therefore all findings must be considered within this context. We selected a well-accepted definition of RV failure/dysfunction that is prognostically and pathologically validated (PAPi < 1.85) in end-stage HF, however, there is no singular accepted definition, and it is possible that this definition misclassified samples. Hemodynamic assessment used to define the status of RV function varied between patients and occurred on average 2–3 weeks before cardiac transplantation. These factors may have led to misclassification by RV function status. To preserve comparability to prior analysis and because this study included a limited number of human samples, we were not able to adjust our analyses for patient characteristics that might introduce bias including age, sex, demographics, or underlying etiology of HF. Subjects with non-ischemic HF are proportionally over-represented among our subgroup of patients with RV failure and there are differences in clinical characteristics between the groups compared, which may impact our findings. Nearly all patients with HF in this study were actively receiving chronic inotropic support with milrinone, which may affect myocardial transcription.

## 4.2 | Conclusions

The RV has a unique transcriptional signature under stress and in failure. Overlapping molecular mechanisms may underlie RV failure in PAH and HF. Fatty Acid metabolism, PPAR signaling, and Adipokine signaling are enriched in the RV compared to the LV and may be promising pathways for RV-specific biomarker development. Studies with prospective assessment of RV function are necessary to accurately define the molecular processes associated with the progression from RV compensation to failure.

### Author Contributions

J.D.G., G.E.D., V.A., F.Y., and E.L.B. contributed to study conception and design. Y.R.S., K.T., and T.A. performed data acquisition. J.D.G. and G.E.D. performed data analysis and drafted the manuscript. All authors participated in data interpretation, critically reviewed the manuscript, and approved the final manuscript submitted for publication.

### Acknowledgments

The Vanderbilt VANTAGE Core provided technical assistance for this study. VANTAGE is supported in part by CTSA Grant (5UL1 RR024975-03), the Vanderbilt Ingram Cancer Center (P30 CA68485), the Vanderbilt Vision Center (P30 EY08126), and NIH/NCRR (G20 RR030956). Myocardial samples were obtained from the Vanderbilt Cardiology Core Laboratory for Translational and Clinical Research. This study was supported by the National Heart Lung and Blood Institute: T32 HL 087738 (Garry), U01 HL125212-01 (Hemnes), R01 HL155278 (Brittain), R34 HL173389 (Brittain), R61/R33 HL 158941 (Brittain), R01 HL163960 (Brittain), R01 HL146588 (Brittain), the US Food and Drug Administration R01 FD007627 (Brittain, Hemnes), American Heart Association Strategically Focused Research Network (SFRN) grant 18SFRN34110369 (Davogustto), American Heart Association 24CDA1271003 (Davogustto), and Veterans Affairs Career Development Award IK2BX005828 (Agrawal).

### Ethics Statement

This study was approved by an institutional review board.

### Consent

Informed consent was obtained from subjects with heart failure and the legally authorized representatives of control donors.

### Conflicts of Interest

The authors declare no conflicts of interest.

### References

1. S. Ghio, C. Raineri, L. Scelsi, M. Ašanin, M. Polovina, and P. Seferovic, “Pulmonary Hypertension and Right Ventricular Remodeling in HFpEF and HFrEF,” *Heart Failure Reviews* 25, no. 1 (2020): 85–91.
2. T. Damy, A. Kallvikbacka-Bennett, K. Goode, et al., “Prevalence of, Associations With, and Prognostic Value of Tricuspid Annular Plane Systolic Excursion (TAPSE) Among Out-Patients Referred for the Evaluation of Heart Failure,” *Journal of Cardiac Failure* 18, no. 3 (2012): 216–225.
3. T. M. Gorter, E. S. Hoendermis, D. J. van Veldhuisen, et al., “Right Ventricular Dysfunction in Heart Failure With Preserved Ejection Fraction: A Systematic Review and Meta-Analysis,” *European Journal of Heart Failure* 18, no. 12 (2016): 1472–1487.



4. A. Raina and T. Meeran, "Right Ventricular Dysfunction and Its Contribution to Morbidity and Mortality in Left Ventricular Heart Failure," *Current Heart Failure Reports* 15, no. 2 (2018): 94–105.
5. M. A. Konstam, M. S. Kiernan, D. Bernstein, et al., "Evaluation and Management of Right-Sided Heart Failure: A Scientific Statement From the American Heart Association," *Circulation* 137, no. 20 (2018): e578–e622.
6. B. A. Houston, E. L. Brittain, and R. J. Tedford, "Right Ventricular Failure," *New England Journal of Medicine* 388, no. 12 (2023): 1111–1125.
7. R. Al-Qazazi, P. D. A. Lima, S. Z. Prisco, et al., "Macrophage-NLRP3 Activation Promotes Right Ventricle Failure in Pulmonary Arterial Hypertension," *American Journal of Respiratory and Critical Care Medicine* 206, no. 5 (2022): 608–624.
8. E. Soon, A. M. Holmes, C. M. Treacy, et al., "Elevated Levels of Inflammatory Cytokines Predict Survival in Idiopathic and Familial Pulmonary Arterial Hypertension," *Circulation* 122, no. 9 (2010): 920–927.
9. L. Jurida, S. Werner, F. Knapp, et al., "A Common Gene Signature of the Right Ventricle in Failing Rat and Human Hearts," *Nature Cardiovascular Research* 3, no. 7 (2024): 819–840.
10. A. L. Frump, M. Albrecht, B. Yakubov, et al., "17 $\beta$ -Estradiol and Estrogen Receptor  $\alpha$  Protect Right Ventricular Function in Pulmonary Hypertension via BMPR2 and Apelin," *Journal of Clinical Investigation* 131, no. 6 (2021): e129433.
11. G. L. Baird, C. Archer-Chicko, R. G. Barr, et al., "Lower DHEA-S Levels Predict Disease and Worse Outcomes in Post-Menopausal Women With Idiopathic, Connective Tissue Disease- and Congenital Heart Disease-Associated Pulmonary Arterial Hypertension," *European Respiratory Journal* 51, no. 6 (2018): 1800467.
12. S. Z. Prisco, T. Thenappan, and K. W. Prins, "Treatment Targets for Right Ventricular Dysfunction in Pulmonary Arterial Hypertension," *JACC: Basic to Translational Science* 5, no. 12 (2020): 1244–1260.
13. E. L. Brittain, M. Talati, J. P. Fessel, et al., "Fatty Acid Metabolic Defects and Right Ventricular Lipotoxicity in Human Pulmonary Arterial Hypertension," *Circulation* 133, no. 20 (2016): 1936–1944.
14. F. Khassafi, P. Chelladurai, C. Valasarajan, et al., "Transcriptional Profiling Unveils Molecular Subgroups of Adaptive and Maladaptive Right Ventricular Remodeling in Pulmonary Hypertension," *Nature Cardiovascular Research* 2, no. 10 (2023): 917–936.
15. R. O. Ramirez Flores, J. D. Lanzer, C. H. Holland, et al., "Consensus Transcriptional Landscape of Human End-Stage Heart Failure," *Journal of the American Heart Association* 10, no. 7 (2021): e019667.
16. T. G. Di Salvo, K. C. Yang, E. Brittain, T. Absi, S. Maltais, and A. Hemnes, "Right Ventricular Myocardial Biomarkers in Human Heart Failure," *Journal of Cardiac Failure* 21, no. 5 (2015): 398–411.
17. Y. Guo, F. Ye, Q. Sheng, T. Clark, and D. C. Samuels, "Three-Stage Quality Control Strategies for DNA Re-Sequencing Data," *Briefings in Bioinformatics* 15, no. 6 (2014): 879–889.
18. Y. Guo, S. Zhao, Q. Sheng, et al., "Multi-Perspective Quality Control of Illumina Exome Sequencing Data Using Qc3," *Genomics* 103, no. 5–6 (2014): 323–328.
19. D. Kim, G. Pertea, C. Trapnell, H. Pimentel, R. Kelley, and S. L. Salzberg, "TopHat2: Accurate Alignment of Transcriptomes in the Presence of Insertions, Deletions and Gene Fusions," *Genome Biology* 14, no. 4 (2013): R36.
20. Z. Bayram, C. Dogan, S. C. Efe, et al., "Prognostic Importance of Pulmonary Artery Pulsatility Index and Right Ventricular Stroke Work Index in End-Stage Heart Failure Patients," *Cardiology* 147, no. 2 (2022): 143–153.
21. K. J. Morine, M. S. Kiernan, D. T. Pham, V. Paruchuri, D. Denofrio, and N. K. Kapur, "Pulmonary Artery Pulsatility Index is Associated With Right Ventricular Failure After Left Ventricular Assist Device Surgery," *Journal of Cardiac Failure* 22, no. 2 (2016): 110–116.
22. S. M. Kochav, R. J. Flores, L. K. Truby, and V. K. Topkara, "Prognostic Impact of Pulmonary Artery Pulsatility Index (PAPi) in Patients With Advanced Heart Failure: Insights From the ESCAPE Trial," *Journal of Cardiac Failure* 24, no. 7 (2018): 453–459.
23. M. I. Aslam, V. Jani, B. L. Lin, et al., "Pulmonary Artery Pulsatility Index Predicts Right Ventricular Myofilament Dysfunction in Advanced Human Heart Failure," *European Journal of Heart Failure* 23, no. 2 (2021): 339–341.
24. M. I. Love, W. Huber, and S. Anders, "Moderated Estimation of Fold Change and Dispersion for RNA-Seq Data With Deseq. 2," *Genome Biology* 15, no. 12 (2014): 550.
25. J. M. Elizarr Ar As, Y. Liao, Z. Shi, et al., "Webgestalt 2024: Faster Gene Set Analysis and New Support for Metabolomics and Multi-Omics," *Nucleic Acids Research* 1, no. 1256879 (2013): 13–14.
26. J. F. Park, V. R. Clark, S. Banerjee, et al., "Transcriptomic Analysis of Right Ventricular Remodeling in Two Rat Models of Pulmonary Hypertension: Identification and Validation of Epithelial-to-Mesenchymal Transition in Human Right Ventricular Failure," *Circulation: Heart Failure* 14, no. 2 (2021): E007058.
27. J. B. Mendelson, J. D. Sternbach, M. J. Doyle, et al., "Multi-Omic and Multispecies Analysis of Right Ventricular Dysfunction," *Journal of Heart and Lung Transplantation* 43, no. 2 (2024): 303–313.
28. L. Jurida, S. Werner, F. Knapp, et al., "A Common Gene Signature of the Right Ventricle in Failing Rat and Human Hearts," *Nature Cardiovascular Research* 3, no. 7 (2024): 819–840.
29. O. Boucherat, T. Yokokawa, V. Krishna, et al., "Identification of LTBP-2 as a Plasma Biomarker for Right Ventricular Dysfunction in Human Pulmonary Arterial Hypertension," *Nature Cardiovascular Research* 1, no. 8 (2022): 748–60.
30. M. H. Talati, E. L. Brittain, J. P. Fessel, et al., "Mechanisms of Lipid Accumulation in the Bone Morphogenetic Protein Receptor Type 2 Mutant Right Ventricle," *American Journal of Respiratory and Critical Care Medicine* 194, no. 6 (2016): 719–728.
31. T. Kobayashi, J. D. Kim, A. Naito, et al., "Multi-Omics Analysis of Right Ventricles in Rat Models of Pulmonary Arterial Hypertension: Consideration of Mitochondrial Biogenesis by Chrysin," *International Journal of Molecular Medicine* 49, no. 5 (2022): 69.
32. J. L. Williams, O. Cavus, E. C. Loccoch, et al., "Defining the Molecular Signatures of Human Right Heart Failure," *Life Sciences* 196 (2018): 118–126.
33. M. K. Friedberg and A. N. Redington, "Right Versus Left Ventricular Failure," *Circulation* 129, no. 9 (2014): 1033–1044.
34. V. Agrawal, T. Lahm, G. Hansmann, and A. R. Hemnes, "Molecular Mechanisms of Right Ventricular Dysfunction in Pulmonary Arterial Hypertension: Focus on the Coronary Vasculature, Sex Hormones, and Glucose/Lipid Metabolism," *Cardiovascular Diagnosis and Therapy* 10, no. 5 (2020): 1522–1540.
35. G. D. Lopaschuk, Q. G. Karwi, R. Tian, A. R. Wende, and E. D. Abel, "Cardiac Energy Metabolism in Heart Failure," *Circulation Research* 128, no. 10 (2021): 1487–1513.
36. M. E. Sweet, A. Cocciolo, D. Slavov, et al., "Transcriptome Analysis of Human Heart Failure Reveals Dysregulated Cell Adhesion in Dilated Cardiomyopathy and Activated Immune Pathways in Ischemic Heart Failure," *BMC Genomics* 19, no. 1 (2018): 812.
37. C. Basu, P. L. Cannon, C. P. Awgulewitsch, C. L. Galindo, E. R. Gamazon, and A. K. Hatzopoulos, "Transcriptome Analysis of Cardiac Endothelial Cells After Myocardial Infarction Reveals Temporal Changes and Long-Term Deficits," *Scientific Reports* 14, no. 1 (2024): 9991.
38. Q. Xiao, N. Hou, Y. P. Wang, et al., "Impaired Sonic Hedgehog Pathway Contributes to Cardiac Dysfunction in Type 1 Diabetic Mice

With Myocardial Infarction,” *Cardiovascular Research* 95, no. 4 (2012): 507–516.

39. H. Kawagishi, J. Xiong, I. I. Rovira, et al., “Sonic Hedgehog Signaling Regulates the Mammalian Cardiac Regenerative Response,” *Journal of Molecular and Cellular Cardiology* 123 (2018): 180–184.

40. M. W. Gorr, K. Sriram, A. M. Chinn, A. Muthusamy, and P. A. Insel, “Transcriptomic Profiles Reveal Differences Between the Right and Left Ventricle in Normoxia and Hypoxia,” *Physiological Reports* 8, no. 2 (2020): e14344.

41. S. P. Murphy, R. Kakkar, C. P. McCarthy, and J. L. Januzzi, “Inflammation in Heart Failure,” *Journal of the American College of Cardiology* 75, no. 11 (2020): 1324–1340.

42. L. Adamo, C. Rocha-Resende, S. D. Prabhu, and D. L. Mann, “Reappraising the Role of Inflammation in Heart Failure,” *Nature Reviews Cardiology* 17, no. 5 (2020): 269–285.

43. Q. L. Nguyen, K. Rao, J. C. Sembrat, et al., “Differential Bioenergetics in Adult Rodent Cardiomyocytes Isolated From the Right Versus Left Ventricle,” *Journal of Molecular and Cellular Cardiology* 190 (2024): 79–81.

### Supporting Information

Additional supporting information can be found online in the Supporting Information section.